Superhydrophilic-Superhydrophobic Patterned Surfaces on Glass Substrate for Water Harvesting

Jichao Zhang[a,#], Faze Chen[b,#], Yao Lu[c], Zhongtao Zhang[a], Jiyu Liu[a], Yang Chen[a], Xin Liu[a,*], Xiaolong Yang[d,*], Claire J. Carmalt[e], Ivan P. Parkin[e]

[a] Key Laboratory for Precision and Non-traditional Machining Technology of the Ministry of Education, Dalian University of Technology, Dalian 116024, P. R. China.

[b] Key Laboratory of Mechanism Theory and Equipment Design of Ministry of Education, Tianjin University, Tianjin 300072, China.

[c.]Department of Chemistry, School of Biological and Chemical Sciences, Queen Mary University of London, London E1 4NS, UK.

[d.]National Key Laboratory of Science and Technology on Helicopter Transmission, Nanjing University of Aeronautics and Astronautics, Nanjing 210016, PR China.

[e] Department of Chemistry, University College London, 20 Gordon Street, London, WC1H 0AJ, UK

Abstract

Directional water harvesting is a special ability of flora and fauna in nature. Wettability-patterned surfaces inspired by natural structures have been extensively researched, and could be a great potential avenue for easing water shortage. However, preparation strategies for these nature-inspired cases, including UV irradiation with mask technology, femtosecond laser direct writing and chemical treatment are time-consuming, cost-ineffective and environmentally unfriendly. In this paper, robust and durable superhydrophobic (SHB) glass substrate was prepared by using laser-induced backward transfer (LIBT) technique and fluoroalkylsilane (FAS) modification. Then wedge-shaped superhydrophilic (SHL) patterns on the SHB surfaces were rapidly constructed by inexpensive and commercially available fiber laser ablation for fog harvesting. This facile, cost effective, and non-corrosive preparation method described herein could be an alternative way to construct SHL-SHB patterns on glass substrate, which could be used for microfluidic devices, droplet manipulation and cell screening.

Keywords: Laser-induced backward transfer; Fiber laser ablation; Superhydrophilic-Superhydrophobic patterns; fog harvesting.

1 Introduction

Water harvesting is a special ability of flora and fauna in nature [1.2]. For example, Namib Desert beetles could live in arid environment due to water harvesting on their back exoskeleton where waxy hydrophobic and non-waxy hydrophilic regions are alternately distributed [3]. Various extremely drought-tolerant plants like cactaceae species could survive in the desert with great fog harvesting performance via well-distributed conical spines and trichomes on their surfaces [4-7]. Likewise, spider silk also possesses excellent water harvesting ability because of unique fibre structures of spindle-knots and joints [8-10]. These natural cases inspired research focusing on construction of wettability-patterned surfaces or special structures to collect water, which shows great potential to alleviate water scarcity in terms of regional water shortage [11].

Wettability-patterned surfaces have been extensively created by mask-based methods. For example, Lin et al. [12] deposited copper on a polyethylene terephthalate (PET) surface via mask-assisted sputtering and then obtained superhydrophilic (SHL) wedge-shaped tracks on the PET substrates by alkali-assisted copper oxidation. The as-prepared patterned surface showed high water harvesting efficiency. Song et al. [13] proposed a mask-assisted chemical etching method to create superhydrophobic (SHB)-SHL patterns on various metal substrates for fog harvesting. Yang et al. [14] described a double electrochemical etching and boiling-water immersion method to fabricate SHL-SHB wedge-shaped pattern on Al substrate with the assistance of masks for fog harvesting. The aforementioned works demonstrated enhanced water harvesting

* Corresponding author. *Email address*: *xinliu@dlut.edu.cn, xlyang@nuaa.edu.cn*

J. Zhang and F. Chen contribute equally.

performance of wettability-patterned surface, but these reported methods involve the use of masks and corrosive chemical solutions, suffering from low processing efficiency and large environmental impact.

Glass substrates are widely used in various fields, such as houses and automobiles, where frequent fog condensate could be observed. Therefore, it should be of great importance to create extreme wettability patterns on glass surface to improve its water harvesting performance. Several methods, including hydrofluoric acid etching [15.16] and laser direct writing (LDW) [17-23], have been proposed to texture glass substrates. LDW is considered as a rapid, green and highly-efficient non-contact machining method. Laser-induced backward transfer (LIBT) is a LDW technology that could realize material deposition on transparent receiver substrates from donor substrates [24-27], thus it could be an alternative tool to create special surface structures on glass substrate for further wettability control. However, to the best of our knowledge, LIBT has been rarely employed to impart glass substrate super-wettability.

In this paper, we firstly obtained robust and durable superhydrophobic glass substrate by using LIBT technique and fluoroalkylsilane (FAS) modification. Then wedge-shaped superhydrophilic patterns on the superhydrophobic surfaces were rapidly constructed by laser ablation. The as-prepared SHL-SHB patterned surface shows impressive fog harvesting ability with an efficiency of 15.68 $mg \cdot cm^{-2} \cdot min^{-1}$. Compared to the reported previous literatures, our work possesses a high water collection efficiency with this facile, cost effective, and non-corrosive preparation method.

2 Experimental Section

2.1 Fabrication of SHL-SHB patterns on glass substrate.

As illustrated in Figure.1, deionized water cleaned slide glass (70 mm × 25 mm × 1 mm) was placed on the metal sheet of aluminum (Al) with a gap of d_{GA}, which could be regulated by commercial tape (thickness of 0.05 mm, DELI Group Co., Ltd). An inexpensive and commercially available fibre laser system (SK-CX30, SK-Marker, China) was used for the LIBT technique to process the glass surface according to circular array pattern (diameter: 100 μm, spacing: 200 μm) with an area of 45 mm × 25 mm at ambient atmospheric pressure and room temperature. The process parameters included a frequency of 20 kHz, a scanning speed of 2000 mm/s, a laser fluence of 318.5 J/cm^2, a pulse width of 100 ns, a focal diameter of 10 μm (focal length *f*: 19.45cm) and an optical wavelength of 1064 ± 5 nm. Then the metal deposited glass surface was modified by 1 wt% fluoroalkylsilane (FAS, $C_8F_{13}H_4Si(OCH_2CH_3)_3$) ethanol solution to obtain a SHB surface. Fibre laser ablation was further conducted to form various complex SHL-SHB patterns on the glass substrate with the same process parameters as the LIBT technique.

Figure 1. Illustration of preparing the SHL-SHB pattern on glass substrate.

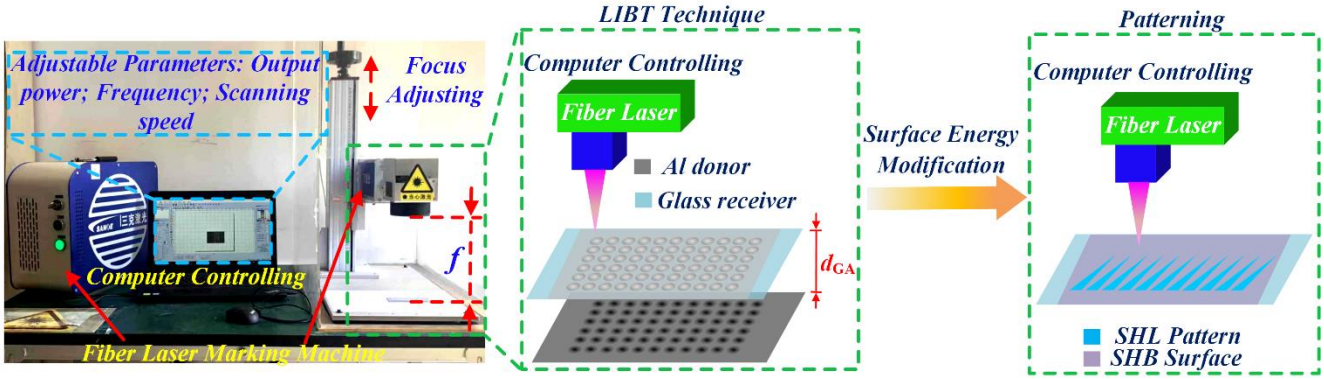

2.2 Robustness and durability test.

Falling sand abrasion and UV irradiation were conducted to test the robustness and durability of the prepared SHB surfaces, respectively. Sand grains (100 g, 0.3 to 0.9 mm in diameter) impinged on the tilted surfaces (45°) from a height of 25 cm with 7 cycles; prepared SHB samples were exposed to UV light (365 nm) for 24 h. Among the aforementioned tests, water contact angle (WCA) and sliding angle (SA) were measured. Tape peeling and fingerprint tests were carried out to investigate robustness of the SHB surfaces.

2.3 Characterization

Water droplets of ~5 μL on samples were recorded by measurement (Krüss, DSA100, Germany) at ambient temperature, from which an average value was calculated from five different positions. The electron microscope (TV-60, China) was used

to observe the variation of surfaces prepared by different gap distances d_{GA} and output powers. The morphology and chemical element distribution were further observed by a scanning electron microscopy equipped with energy-dispersive X-ray (SEM & EDX, SUPRA 55 SAPPHIRE, Germany). Chemical composition was further characterized by an X-ray diffractometer (XRD, Empyrean, Holland, X-ray source (Cu Kα radiation (k = 0.15418 nm)) within the 5-100° range at a scanning rate of 2θ = 0.026 °/min and X-ray photoelectron spectroscopy (XPS, Thermo ESCALAB250Xi, American). Curve fitting of C 1s peak was operated by XPS peak 4.1 software with the C 1s peak at 284.6 eV as a reference.

2.4 Fog harvesting.

To extend the application of SHL-SHB pattern on glass substrate, the pattern of wedge-shaped tracks (wedge angle of 7°) was prepared for harvesting of the fog condensate. In a fog harvesting test (temperature: 20 ± 1°C, RH: 80 ± 5%), the surfaces, including bare SHL, untreated glass, pristine Al surface, bare SHB, and patterned glass, were vertically fixed at the holder. The culture dish was placed under the prepared sample for fog harvesting, as shown in Figure 2. Fog was simulated by a household humidifier (ultrasonic nebulizer402Al, moisture flow: ~3 mL/min), with a distance of 50 mm between the prepared surface and nozzle of the fog generator. Precision balance (resolution: 0.1 mg) was used to weigh the collected water for 20 min. A Sony camera (DSC-RX10M3, Japan) was used to record the aforementioned processes.

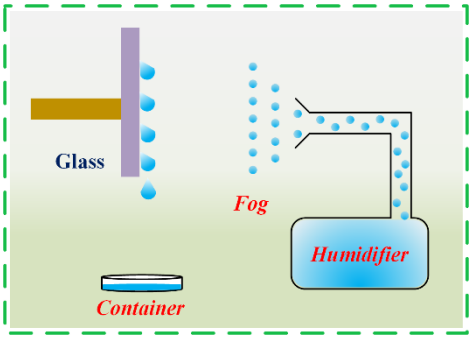

Figure 2. Illustration of fog harvesting

3 Results and discussion

3.1 Fabrication of extreme wetting patterns on an Al plate

The influences of gap distance d_{GA} and output power on water contact angle (WCA) and sliding angle (SA) of the glass surface were firstly evaluated. As shown in Figure 3 a1-a4 and b1-b4, the gap distance from 0.15 mm to 0.55 mm could all be used to obtain a SHB surface, where WCAs remained above 150° under the different output power from 0.3 W to 7.5 W, compared to untreated glass (19 °) and pristine Al (70 °). However, it was obvious that SAs would decrease with the descent of the gap d_{GA}, among which the SA of SHB surface prepared by d_{GA} of 0.15 mm and output power of 7.5 W reached 0° and water droplet could easily roll off from the 0-degree plane (Movie S1 and Figure S1 in the Supplementary Information). In addition, this surface also manifested more uniform morphology, as shown in Figure S2 of Supplementary Material, indicating that the surface was better treated compared with others. Furthermore, by fixing the output power of 7.5 W, samples prepared by d_{GA} of 0 mm, 0.05 mm and 0.10 mm were then used to investigate the enhanced influence of d_{GA} as shown in Figure 3c. However, it was found that the glass receiver was bound to the donor Al substrate, which was inapplicable for further large-scale fabrication by LIBT technique due to instability in preparation. According to previous literature [28], the processes of the LIBT technique can be attributed to donor material melting, vaporizing and ultimately depositing on the rear of the transparent glass receiver, facing the Al sheet. Thus, with the decrease of d_{GA}, the intensive function of the LIBT processes would happen, resulting in the glass and Al sheet bonding together. Therefore, preparation parameters were fixed with d_{GA} of 0.15 mm and output power of 7.5 W, unless specified otherwise.

Due to the practical influence of sand-wind weather and the irradiation of sunlight, SHB glass substrate requires investigation for robustness and durability test by falling sand abrasion and UV irradiation. As illustrated in Figure 4a-b and Movie S2 of Supplementary Material, the red dyed droplet was observed to rapidly roll off from the tilted surface after the test. WCAs changed from 165° ± 3.1° to 155° ± 5.4° during 6 cycles test and finally dropped to approximate 147° after 7

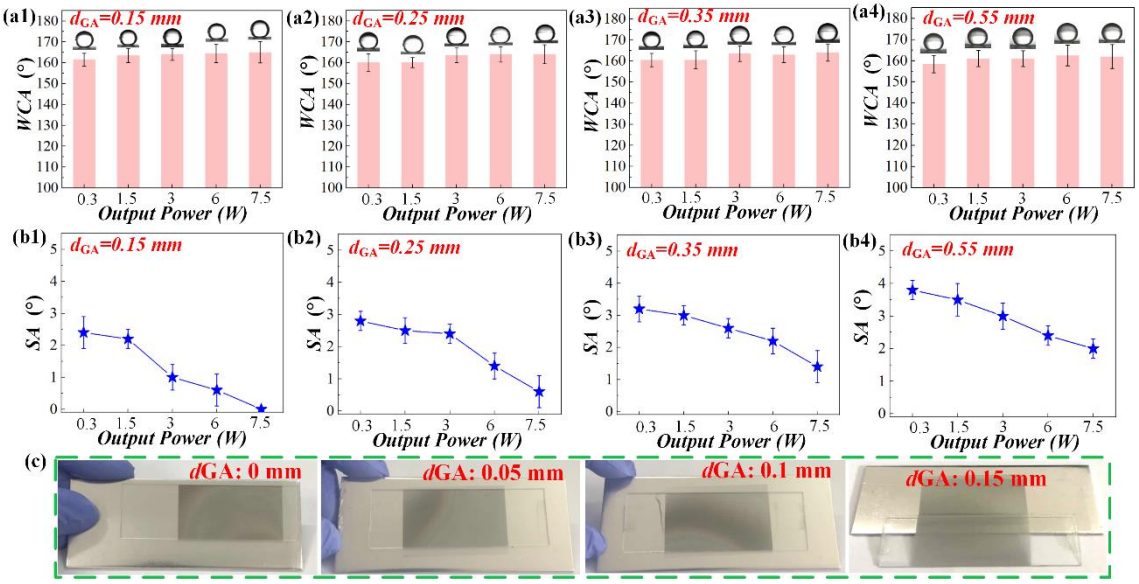

Figure 3. WCAs (a1-a4) and SAs (b1-b4) of SHB surface on glass substrate fabricated by LIBT technique under the gap distance d_{GA} of 0.15 mm, 0.25 mm, 0.35 mm, 0.55 mm with different output powers. (c) influence of different gap distances (d_{GA}) under the output power of 7.5 W.

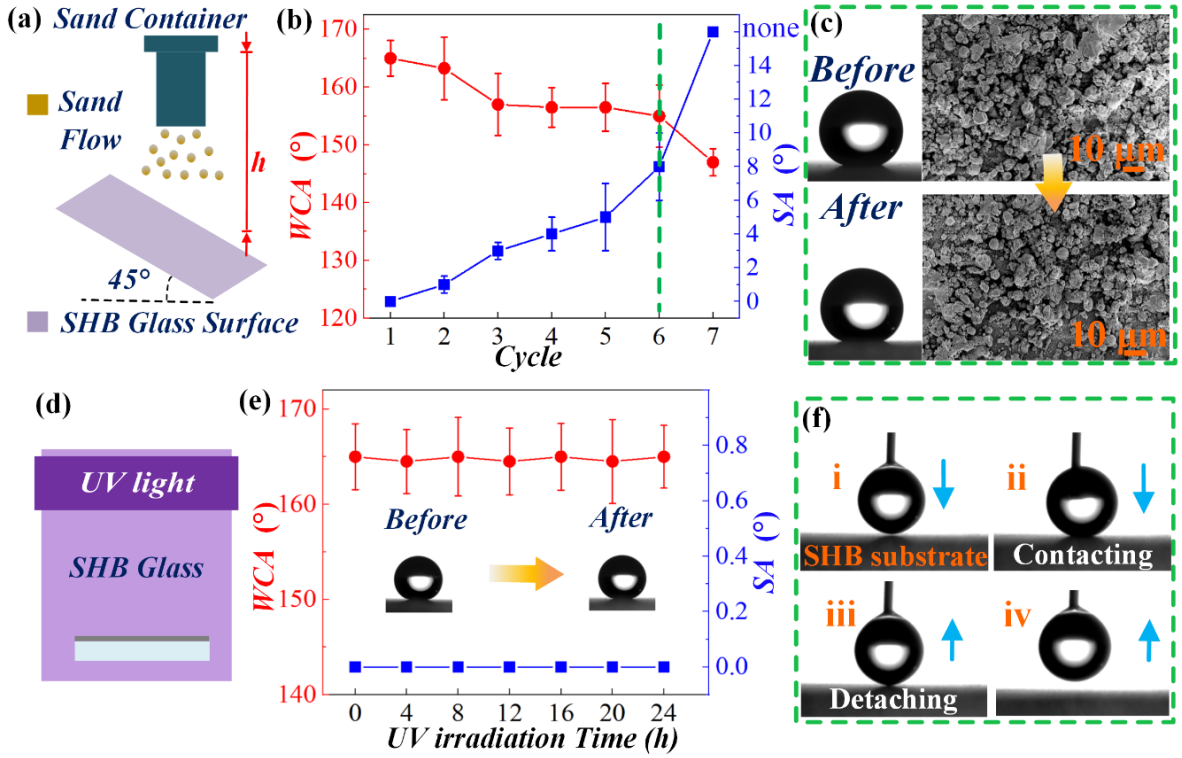

Figure 4. Robustness and durability test of the SHB surface. (a-b) falling sand abrasion test and measured WCAs and SAs of 7 cycles. (c) the morphology of SHB surface before and after 6 cycles falling sand abrasion test. (d-e) UV resistance test and measured WCAs and SAs of 24 h. (f) Process of contacting and detachment on UV irritated SHB glass surface.

cycles. In addition, SAs remained less than 10° during 6 cycles test while water droplet could not roll off after the 7th cycle, demonstrating robustness of SHB surface during 6 cycles falling sand test. It can be seen from the SEM images that little variation was found before and after the 6 cycles test, as shown in Figure 4c. For the examination of UV resistance, the WCA still remained at 165 ± 3.3° after 24 h UV exposure, as shown in Figure 4d-e. When the droplet contacted the UV irritated SHB glass surface, easy detachment from SHB substrate could be observed, as shown in Figure 4f. It was observed that the water droplets could still roll down from the surfaces after these tests including tape peeling and fingerprint tests, as shown in Movies S3 and S4 of Supplementary Information, demonstrating its good mechanical strength [29].

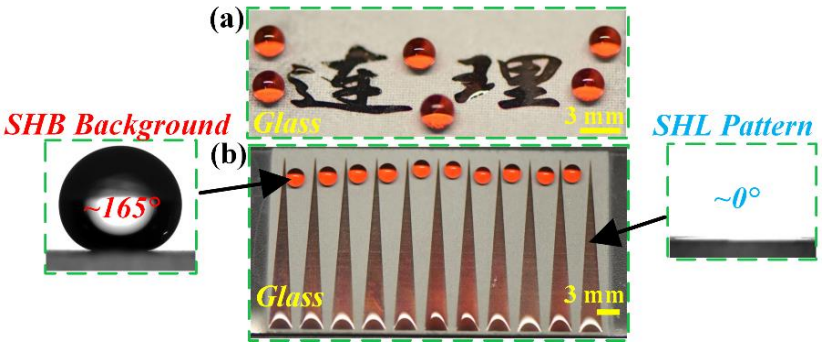

Figure 5. SHL-SHB pattern on glass substrate. (a) Chinese character. (b) wedge-shaped tracks.

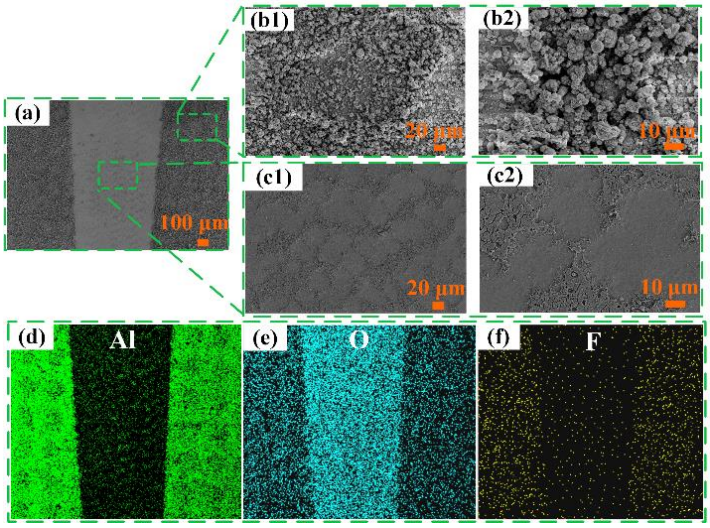

Figure 6. Characterization of the SHL-SHB pattern on glass substrate. (a) SEM image. (b1-b2) SHB untreated area. (c1-c2) laser treated area. SEM-EDX mappings of the surface with elements (d) Al, (e) O, (f) F.

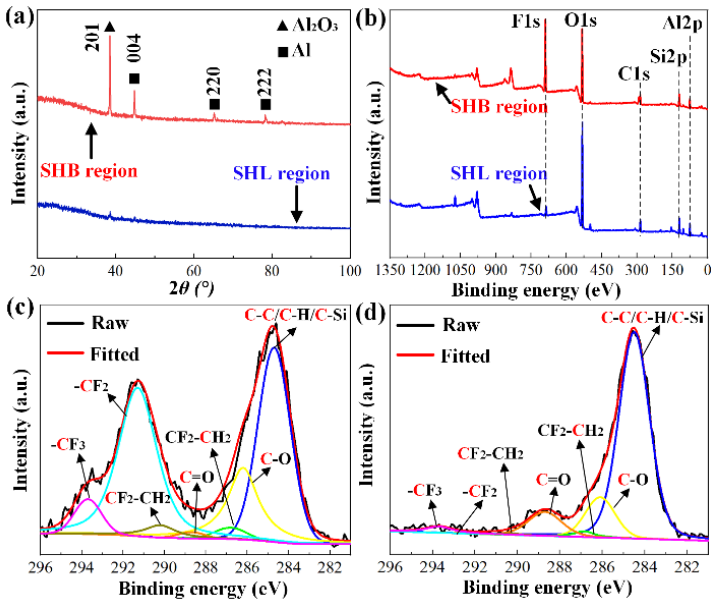

Figure 7. Characterization of morphologies and chemical composition of the SHL-SHB pattern on glass substrate. (a) XRD patterns of SHB region and SHL region. (b) XPS spectra of elements. Peak-fitted high-resolution C 1s spectra of (c) SHB region and (d) SHL region.

As a facile, green and rapid preparation method, inexpensive and commercially available fibre laser ablation was used to construct various complex SHL-SHB patterns such as Chinese characters, wedge-shaped tracks and folding fan pattern, as shown in Figure 5a-b and Figure S3a of the Supplementary Material. SHL-SHB pattern was further characterized by SEM, as shown in Figure 6a. Treated surface on glass substrate was characterized with hierarchical structures on the SHB area compared to the relative smooth morphologies of laser treated area, demonstrating the function of laser ablation, as shown in

Figure. 6 b1-b2 and c1-c2. The EDX elemental mapping of the patterned surface displayed the depletion of aluminum content (Figure. 6d), enrichment of oxygen content (Figure. 6e) and depletion of fluorine content (Figure 6f), which confirmed a selective patterning by laser ablation for creating a SHL-SHB patterned glass substrate.

Furthermore, from the XRD patterns of SHB region and SHL region, as shown in Figure 7a, the diffraction peaks were assigned to Al_2O_3 and Al and referenced to JCPDS Card No. 052-0803 and No. 04-0787, respectively. The XRD pattern and cross-sectional view (Figure S3b of Supplementary Material) of the SHB region indicated that the glass surface was successfully deposited by donor materials during the process of the LIBT technique. After laser ablation treatment, most of the deposited layer were removed according to XRD pattern of SHL region. XPS spectra were also used to investigate the chemical composition of SHB untreated area and laser ablated area as depicted in Figure 7b, which were mainly composed of C 1s, O 1s, F 1s, Al 2p, and Si 2p. The relative contents of O and F changed before and after laser treatment. For the SHB region, the relative contents of O and F were 34.3 and 24.6 at.%, respectively. At the SHL region, the O content increased to 49.0 at.%, while the F content plunged to 3.8 at.%, as shown in Figure S4 of Supplementary Material. Thus, the composition variation accounts for the patterned surfaces with wettability contrast. Figure 7c-d shows the high-resolution C 1s peaks fitting results of the SHB region and the SHL region, which was deconvoluted into seven components including C-C bonds together with C-H and C-Si, which was centred at 284.6 ± 0.14 eV. The components at 286.1 ± 0.07 eV and 286.8 ± 0.03 eV were respectively attributed to C-O and CF_2-$\underline{C}H_2$ groups. The C=O group contribution was found at 288.6 ± 0.01 eV. A binding energy of 290.3 ± 0.07 eV was attributed to CF_2-CH_2 group. The peaks at 291.3 ± 0.01 eV and 293.7 ± 0.01 eV were assigned to -CF_2 and terminal -CF_3 moieties, respectively [30.31]. As summarized in Table S1 of Supplementary Material, the SHB region contained about 37.6% -CF_2 and 5.0% -CF_3. In contrast, after laser ablation, the contents of -CF_2 and -CF_3 decreased to 0.2% and 2.6%, respectively, while C=O increased from 0.9% to 9.2%. Consequently, laser ablation treatment could rapidly obtain the observed SHL patterns on a SHB surface due to the reduction of hydrophobic F-containing groups and the increment of the hydrophilic O-containing groups.

Inspired by the contrast wettability structures of the desert beetle [32], the prepared samples were firstly used for fog harvesting. As shown in Figure 8a-b, it was obvious that condensing water droplet grew, merged into a larger droplet and finally formed a huge bump at the bottom of surface of the untreated glass and pristine (Movie S5 and S6 of Supplementary Material). While in contrast, as shown in Figure 8c, the bare SHL background manifested great fog adsorption capacity with water condensates spreading rapidly and forming film-like condensation areas in only 19 s. However, with a low rate of droplets proceeding, a huge bump was observed after water flowed downwards (Movie S7 of Supplementary Material). For bare SHB background shown in Figure 8d, dropwise condensation took place with condensing droplets growing, contacting with each other, merging into a large droplet and falling off from the surface (Movie S8 of Supplementary Material). By contrast, for wedge shaped SHL-SHB pattern 1 (SSP_1) with spacing distance of d_1 (4 mm), nucleated droplet constantly grew and merged at SHB regions which were transported into SHL domains after contacting the border of SHL pattern. Driven by inner Laplace pressure gradient [33-36], pumpless transportation of the condensing water took place at the SHL wedge shaped track pattern (Movie S9 of Supplementary Material). As shown in Figure 8e, neighbouring droplets at the tail end of tracks merged into a large droplet due to close spacing distance of 4 mm, demonstrating fast transition to film-like condensation. Wedge shaped SHL-SHB pattern 2 (SSP_2) with spacing distance of d_2 (8 mm) is shown in Figure 8f. However, condensing droplets rapidly shed off due to the gravity force with the droplet volume increasing and reaching the threshold value (Movie S10 of Supplementary Material), decreasing the water residual and realizing sustained droplet drainage.

Water condensates were then collected during fog harvesting for 20 min. For bare SHL background, only one droplet shed off, as shown in Figure 9a. On the untreated glass substrate, pristine Al surface and bare SHB surface, condensing droplets took more time to converge and average departing droplet mass was 91.1 mg, 59.0 mg, and 57.8 mg respectively, which could hardly provide efficient droplet drainage. For the sample of SSP_1 with spacing distance of 4 mm, 15 droplets with average mass of 158.0 mg were collected, which is too large to promote high efficiency of sustained drainage, compared to 70 droplets with average droplet mass of 50.4 mg for the sample of SSP_2 (8 mm). Figure 9b shows bare SHL surface possessed the lowest efficiency of 1.78 $mg \cdot cm^{-2} \cdot min^{-1}$, compared with untreated glass (3.64 $mg \cdot cm^{-2} \cdot min^{-1}$) and pristine Al surface (8.71 $mg \cdot cm^{-2} \cdot min^{-1}$). Due to the great pinning force on the wetted SHB surface, the fog harvesting efficiency was 10.26 $mg \cdot cm^{-2} \cdot min^{-1}$. Influenced by the close spacing distance, SSP_1 (4 mm) exhibited harvesting efficiency of 10.58 $mg \cdot cm^{-2} \cdot min^{-1}$; while spacing distance increased to d_2 (8 mm), condensing droplets could rapidly shed off and realized a new cycle of droplet drainage after growing beyond departing volume and exceeding the pining force of tail end, resulting in the highest fog harvesting efficiency

of 15.68 mg·cm^{-2}·min^{-1}. Compared with bare SHL background, untreated glass, pristine Al, and SHB surface, this impressive fog harvesting ability of SHL-SHB wedge shaped tracks pattern on glass substrate increases the harvesting efficiency by nearly 781%, 331%, 80%, and 53%, respectively. A comparison between our work and the data found in previous literatures is listed in Table S2 of Supplementary Information. It is evident that our work possesses a high water collection efficiency with this facile, cost effective, and non-corrosive preparation method. As shown in Figure 9c, the influence of droplet volume on pumpless transportation was then investigated. When deposited on the front end of the wedge shaped track with the distance of 23 mm, droplets of 35 μL would only took 238 ms to complete the transportation process (Movie S11 of Supplementary Material); while droplets of 5 μL needed 680 ms to complete the process. The results indicated that droplets of 5 μL and 35 μL could both rapidly reach the tail end of track driven by inner Laplace pressure gradient .

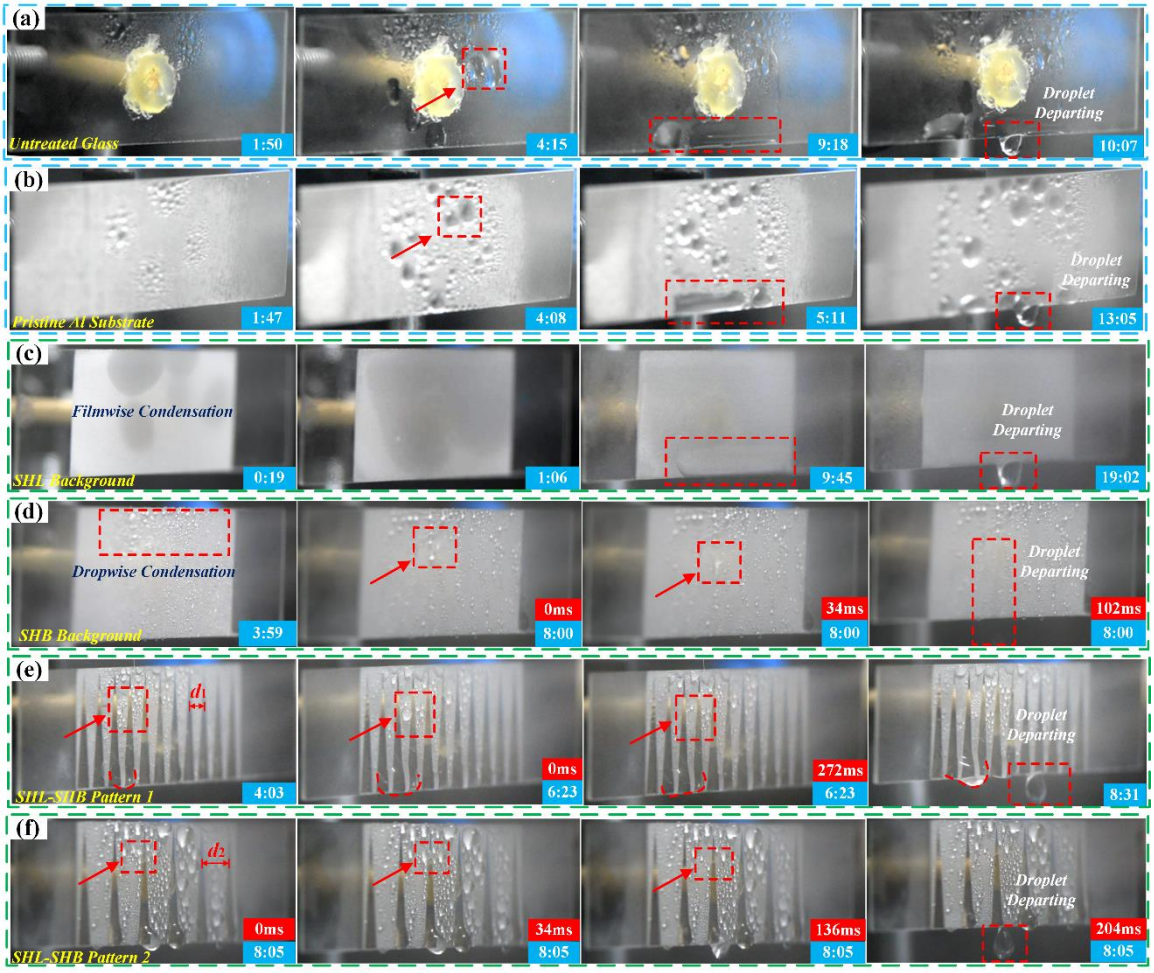

Figure 8. Fog harvesting. (a) untreated glass. (b) pristine Al substrate. (c) SHL background. (d) SHB background. (e) SHL-SHB pattern 1 with spacing distance of d_1. (f) SHL-SHB pattern 2 with spacing distance of d_2.

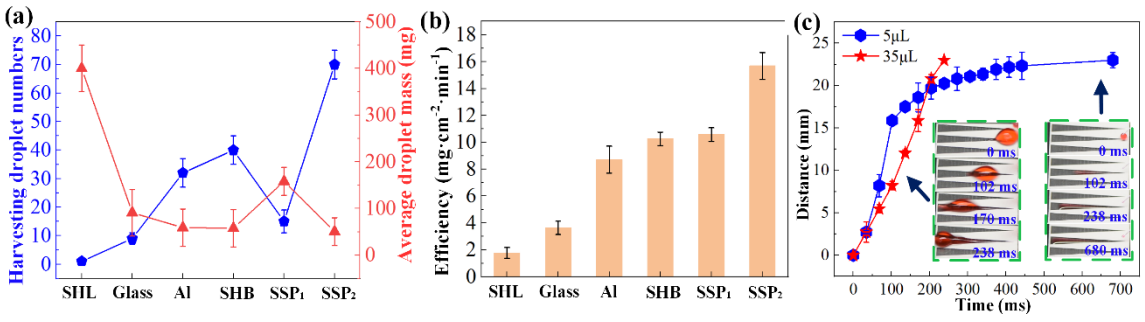

Figure 9. Fog harvesting (a) harvesting droplet numbers and average droplet mass. (b) fog harvesting efficiency. (c) pumpless transportation process.

4. Conclusion

We constructed SHL wedge shaped patterns on robust and durable SHB glass substrates by using the LIBT technique, FAS modification and laser ablation, avoiding the use of mask technology and any hazard chemicals. This research could be an

alternative way SHL-SHB patterns on glass substrates, which is not merely a promising candidate for water harvesting to alleviate he regional water shortage but also for microfluidic devices, droplet manipulation and cell screening.

Acknowledgements

This work was financially supported by the National Natural Science Foundation of China (NSFC, Grant No.51305060); National Basic Research Program of China (grant No.2015CB057304). F. Chen acknowledges the support from National Postdoctoral Program for Innovative Talents (No. BX20190233). I. P. Parkin acknowledges the support from EPSRC grant of Industrial Doctorate Centre: Molecular Modelling & Materials Science (EP/G036675/1). Yao Lu acknowledges the financial support from the QMUL-SBCS start up.

References:

[1] J. Li, J. Li, J. Sun, S. Feng, Z. Wang (2019) Biological and Engineered Topological Droplet Rectifiers., Adv. Mater. 31:1806501.

[2] M. Zhu, Y. Li, G. Chen, F. Jiang, Z. Yang, X. Luo, Y. Wang, S.D. Lacey, J. Dai, C. Wang, C. Jia, J. Wan, Y. Yao, A. Gong, B. Yang, Z. Yu, S. Das, L. Hu (2017) Tree-Inspired Design for High-Efficiency Water Extraction., Adv. Mater. 29:1704107.

[3] A.R. Parker, C.R. Lawrence (2001) Water capture by a desert beetle., Nature 414:33-34.

[4] T. Xu, Y. Lin, M. Zhang, W. Shi, Y. Zheng (2016) High-Efficiency Fog Collector: Water Unidirectional Transport on Heterogeneous Rough Conical Wires., ACS Nano 10:10681-10688.

[5] Y. Peng, Y. He, S. Yang, S. Ben, M. Cao, K. Li, K. Liu, L. Jiang (2015) Magnetically Induced Fog Harvesting via Flexible Conical Arrays., Adv. Funct. Mater. 25:5967-5971.

[6] M. Cao, J. Ju, K. Li, S. Dou, K. Liu, L. Jiang (2014) Facile and Large-Scale Fabrication of a Cactus-Inspired Continuous Fog Collector., Adv. Funct. Mater. 24:3235-3240.

[7] J. Ju, H. Bai, Y. Zheng, T. Zhao, R. Fang, L. Jiang (2012) A multi-structural and multi-functional integrated fog collection system in cactus., Nat Commun 3:1247.

[8] C. Li, Y. Liu, C. Gao, X. Li, Y. Xing, Y. Zheng (2019) Fog Harvesting of a Bioinspired Nanocone-Decorated 3D Fiber Network., ACS Appl Mater Inter 11:4507-4513.

[9] Y. Tian, P. Zhu, X. Tang, C. Zhou, J. Wang, T. Kong, M. Xu, L. Wang (2017) Large-scale water collection of bioinspired cavity-microfibers., Nat Commun 8:1080.

[10] Y. Zheng, H. Bai, Z. Huang, X. Tian, F. Nie, Y. Zhao, J. Zhai, L. Jiang (2010) Directional water collection on wetted spider silk., Nature 463:640-643.

[11] P.B. Bintein, H. Lhuissier, A. Mongruel, L. Royon, D. Beysens (2019) Grooves Accelerate Dew Shedding., Phys. Rev. Lett. 122:98005.

[12] J. Lin, X. Tan, T. Shi, Z. Tang, G. Liao (2018) Leaf Vein-Inspired Hierarchical Wedge-Shaped Tracks on Flexible Substrate for Enhanced Directional Water Collection., ACS Appl Mater Inter 10:44815-44824.

[13] J. Sun, C. Chen, J. Song, J. Liu, X. Yang, J. Liu, X. Liu, Y. Lu (2019) A universal method to create surface patterns with extreme wettability on metal substrates., J. Colloid Interf. Sci. 535:100-110.

[14] X. Yang, J. Song, J. Liu, X. Liu, Z. Jin (2017) A Twice Electrochemical-Etching Method to Fabricate Superhydrophobic-Superhydrophilic Patterns for Biomimetic Fog Harvest., Sci Rep 7:8816.

[15] S. Han, S. Ji, A. Abdullah, D. Kim, H. Lim, D. Lee (2018) Superhydrophilic nanopillar-structured quartz surfaces for the prevention of biofilm formation in optical devices., Appl. Surf. Sci. 429:244-252.

[16] Y. Song, Y. Liu, H. Jiang, S. Li, C. Kaya, T. Stegmaier, Z. Han, L. Ren (2018) Temperature-tunable wettability on a bioinspired structured graphene surface for fog collection and unidirectional transport., Nanoscale 10:3813-3822.

[17] T. Alqurashi, M. Alnufaili, M.U. Hassan, S. Aloufi, A.K. Yetisen, H. Butt (2019) Laser Inscription of Microfluidic Devices for Biological Assays., ACS Appl Mater Inter 11:12253-12260.

[18] V.B. Nam, J. Shin, Y. Yoon, T.T. Giang, J. Kwon, Y.D. Suh, J. Yeo, S. Hong, S.H. Ko, D. Lee (2019) Highly Stable Ni-Based Flexible Transparent Conducting Panels Fabricated by Laser Digital Patterning., Adv. Funct. Mater. 29:1806895.

[19] Y. Lin, J. Han, M. Cai, W. Liu, X. Luo, H. Zhang, M. Zhong (2018) Durable and robust transparent superhydrophobic glass surfaces fabricated by a femtosecond laser with exceptional water repellency and thermostability., J. Mater Chem A 6:9049-9056.

[20] M. Heinz, V.V. Srabionyan, L.A. Avakyan, A.L. Bugaev, A.V. Skidanenko, S.Y. Kaptelinin, J. Ihlemann, J. Meinertz, C. Patzig, M. Dubiel, L.A. Bugaev (2018) Formation of bimetallic gold-silver nanoparticles in glass by UV laser irradiation., J. Alloy. Compd 767:1253-1263.

[21] E. Kostal, S. Stroj, S. Kasemann, V. Matylitsky, M. Domke (2018) Fabrication of Biomimetic Fog-Collecting Superhydrophilic – Superhydrophobic Surface Micropatterns Using Femtosecond Lasers., Langmuir 34:2933-2941.

[22] F.H. Rajab, Z. Liu, L. Li (2018) Production of stable superhydrophilic surfaces on 316L steel by simultaneous laser texturing and SiO_2 deposition., Appl. Surf. Sci. 427:1135-1145.

[23] M. Wang, Q. Liu, H. Zhang, C. Wang, L. Wang, B. Xiang, Y. Fan, C.F. Guo, S. Ruan (2017) Laser Direct Writing of Tree-Shaped Hierarchical Cones on a Superhydrophobic Film for High-Efficiency Water Collection., ACS Appl Mater Inter 9:29248-29254.

[24] U. Zywietz, A.B. Evlyukhin, C. Reinhardt, B.N. Chichkov (2014) Laser printing of silicon nanoparticles with resonant optical electric and magnetic responses., Nat Commun 5:3402.

[25] H. Sakata, S. Chakraborty, M. Wakaki (2012) Patterning of Bi2O3 films using laser-induced forward and backward transfer techniques., Microelectron. Eng. 96:56-60.

[26] N. Mir-Hosseini, M.J.J. Schmidt, L. Li (2005) Growth of patterned thin metal oxide films on glass substrates from metallic bulk sources using a Q-switched YAG laser., Appl. Surf. Sci. 248:204-208.

[27] P. Papakonstantinou, N.A. Vainos, C. Fotakis (1999) Microfabrication by UV femtosecond laser ablation of Pt, Cr and indium oxide thin films., Appl. Surf. Sci. 151:159-170.

[28] G. Dhami, B. Tan, K. Venketakrishnan (2011) Laser induced reverse transfer of gold thin film using femtosecond laser., Opt. Laser. Eng. 49:866-869.

[29] S. Kolkowitz, A. Safira, A.A. High, R.C. Devlin, S. Choi, Q.P. Unterreithmeier, D. Patterson, A.S. Zibrov, V.E. Manucharyan, H. Park, M.D. Lukin (2015) Probing Johnson noise and ballistic transport in normal metals with a single-spin qubit., Science 347:1129-1132.

[30] F. Chen, J. Liu, Y. Cui, S. Huang, J. Song, J. Sun, W. Xu, X. Liu (2016) Stability of plasma treated superhydrophobic surfaces under different ambient conditions., J. Colloid Interf. Sci. 470:221-228.

[31] K. Ellinas, S.P. Pujari, D.A. Dragatogiannis, C.A. Charitidis, A. Tserepi, H. Zuilhof, E. Gogolides (2014) Plasma Micro-Nanotextured, Scratch, Water and Hexadecane Resistant, Superhydrophobic, and Superamphiphobic Polymeric Surfaces with Perfluorinated Monolayers., ACS Appl Mater Inter 6:6510-6524.

[32] P.S. Mahapatra, A. Ghosh, R. Ganguly, C.M. Megaridis (2016) Key design and operating parameters for enhancing dropwise condensation through wettability patterning., Int. J. Heat Mass Tran. 92:877-883.

[33] S. Wang, C. Wang, Z. Peng, S. Chen (2019) Moving Behavior of Nanodroplets on Wedge-Shaped Functional Surfaces., The Journal of Physical Chemistry C 123:1798-1805.

[34] U. Sen, S. Chatterjee, R. Ganguly, R. Dodge, L. Yu, C.M. Megaridis (2018) Scaling Laws in Directional Spreading of Droplets on Wettability-Confined Diverging Tracks., Langmuir 34:1899-1907.

[35] S. Huang, J. Song, Y. Lu, F. Chen, H. Zheng, X. Yang, X. Liu, J. Sun, C.J. Carmalt, I.P. Parkin, W. Xu (2016) Underwater Spontaneous Pumpless Transportation of Nonpolar Organic Liquids on Extreme Wettability Patterns., ACS Appl Mater Inter 8:2942-2949.

[36] J. Song, Z. Liu, X. Wang, H. Liu, Y. Lu, X. Deng, C.J. Carmalt, I.P. Parkin (2019) High-efficiency bubble transportation in an aqueous environment on a serial wedge-shaped wettability pattern., J. Mater Chem A 7:13567-13576.